Simultaneous Acquisition of Quadrupolar Order and Double-Quantum ^{23}Na Signals

K. J. Jung,* P. J. Cannon,* and J. Katz*,†

*Department of Medicine, Division of Cardiology, and †Department of Radiology, College of Physicians and Surgeons,
Columbia University, 630 West 168th Street, New York, New York 10032

Na$^+$ with both residual quadrupolar coupling and biexponential relaxation contributes to the signal acquired from DQF-4, while only Na$^+$ with residual quadrupolar coupling contributes to the signal acquired with the Jeener–Broekaert sequence. Since RF phases and flip angles for DQF-4 and Jeener-Broekaert sequences are identical, these different types of signals can be generated simultaneously. A phase-cycling scheme is developed to differentiate the signals corresponding to residual quadrupolar coupling and biexponential relaxation after the signals are acquired by use of the same RF sequences. This technique can maximize the attainable information from Na$^+$ in biological tissues in a given acquisition time. © 1997 Academic Press

Key Words: ^{23}Na, quadrupolar coupling, biexponential relaxation, double-quantum filtering, Jeener–Broekaert.

INTRODUCTION

Quadrupolar nuclei such as ^{23}Na with biexponential relaxation or nonvanishing quadrupolar coupling can be excited to generate multiple-quantum (MQ) coherence (*1, 2*). MQ filtering (MQF) of ^{23}Na has been applied to biological systems for the suppression of free or unbound Na$^+$ (*3–7*) and the detection of ordered structures in tissues (*8–10*).

In the pulse sequences for conventional MQF, RF phases and flip angles for the generation of MQ signals are exclusive of each other. Thus, it has not been possible to generate MQ signals of different coherence orders simultaneously.

The Jeener–Broekaert (J–B) sequence can produce a signal derived from the quadrupolar order (QO), i.e., T_{20} in an irreducible tensor notation (*11*). Although the QO term represents a spin population, it is represented as a zero-quantum (ZQ) in a mathematical derivation by use of irreducible tensors and reduced rotation matrix elements (*11, 12*). Furthermore, the filtering by RF phases for the QO term is the same as that for ZQ coherence. In this respect, the J–B sequence is included in the general category of MQF here.

This QO term can be generated for Na$^+$ with residual quadrupolar coupling as for Na$^+$ in an ordered structure. The QO signal in the J–B sequence is derived from Na$^+$

with residual quadrupolar coupling. On the other hand, the double-quantum (DQ) signal in DQF-4 is derived mostly from biexponential relaxation, with only part of the contribution from quadrupolar coupling (*12*). Since the RF phases and flip angles for the J–B sequence are identical to those for DQF-4, both QO and DQ signals can be generated by the same RF sequence. Here, a technique to acquire both signals simultaneously and then to separate them into two distinct signals is presented and verified experimentally.

METHODS

The MQF pulse sequence with refocused preparation time (τ_P) and nonrefocused evolution time (τ_E) may be represented by

$$(\theta_1, \phi_1) - \frac{\tau_P}{2} - (\theta_2, \phi_2) - \frac{\tau_P}{2} -$$
$$(\theta_3, \phi_3) - \tau_E - (\theta_4, \phi_4) - \text{Acq}(t_2, \phi_R), \qquad [1]$$

where ϕ_n denotes the phase of each RF pulse with flip angle θ_n, ϕ_R is the receiver phase, and t_2 is the acquisition time. In general, $\theta_1 = \frac{1}{2}\pi$ and $\theta_2 = \pi$.

RF phases and flip angles for J–B, conventional DQ filtering (DQF-1), and triple-quantum filtering (TQF) sequences are summarized in Table 1 (*12*). Here, RF phases ϕ_P and ϕ_E are defined as

$$\phi_P = \phi_1 - 2\phi_2 + \phi_3 \qquad [2]$$

and

$$\phi_E = -\phi_3 + \phi_4. \qquad [3]$$

As shown in Table 1, RF phases and flip angles for these MQF schemes are mutually exclusive; i.e., ϕ_P for DQF-1 is different from that for J–B and TQF, ϕ_E for J–B is different from that for TQF, and θ_3 and θ_4 for J–B are different from those for DQF-1 and TQF. Therefore, each of these MQF

TABLE 1
RF Phases and Flip Angles for J–B, DQF-1, and TQF Sequences

	ϕ_P	ϕ_E	ϕ_R	θ_3	θ_4
J–B	$(k + \frac{1}{2})\pi$	$\frac{n}{2}\pi$	0	$\frac{1}{4}\pi$	$\frac{1}{4}\pi$
DQF-1	$k\pi$	$\frac{n}{2}\pi$	$n\pi$	$\frac{1}{2}\pi$	$\frac{1}{2}\pi$
TQF	$(k + \frac{1}{2})\pi$	$(\frac{n}{3} + \frac{1}{6})\pi$	$n\pi$	$\frac{1}{2}\pi$	$\frac{1}{2}\pi$

Note. k and n are integer variables. n is cycled for the filtering.

sequences cannot be employed to generate different MQ signals simultaneously. Furthermore, it is also clear that sole modification of the receiver phase in the various MQF sequences cannot be employed to differentiate between the various MQ signals.

However, one of the new DQF schemes introduced in Ref. (*12*), i.e., DQF-4, has the identical pulse sequence as J–B, except for the receiver phase in the phase cycling for selection of the coherence order. The RF phases and flip angles for J–B and DQF-4 sequences are summarized in Table 2. Since the RF phases and flip angles are the same for both MQFs, both QO and DQ signals can be generated by the same RF sequence.

The difference between J–B and DQF-4 sequences is in the receiver phase. The receiver phases for J–B and DQF-4 can be denoted as $\phi_R^{(0)}$ and $\phi_R^{(2)}$, respectively. They may be expressed in terms of RF phases as

$$\phi_R^{(0)} = -\phi_P - \phi_4 \qquad [4]$$

and

$$\phi_R^{(2)} = -\phi_P - \phi_4 + 2\phi_E. \qquad [5]$$

For the phase cycling $\phi_E = \frac{1}{2}n\pi$ with an integer variable n as in Table 2, Eq. [5] may be rewritten as

$$\phi_R^{(2)} = -\phi_P - \phi_4 + n\pi. \qquad [6]$$

Note that the receiver phase for J–B is independent of ϕ_E as for ZQ coherence, while that for DQF-4 is a function of $2\phi_E$. Hence, QO and DQ signals can be differentiated by cycling ϕ_E. A straightforward way of separating these two signals is to filter the data after the signals are acquired with cycling of ϕ_E and a constant receiver phase. However, a much more efficient approach which does not require storage for such a large number of FIDs may also be implemented.

The receiver phase $\phi_R^{(2)}$ can be divided into two groups, i.e., even n and odd n. Denoting the MQ signals acquired for the two groups as S_{even} and S_{odd}, respectively, QO (S_{QO})

and DQ (S_{DQ}) signals can be obtained by linear superposition of S_{even} and S_{odd} as

$$S_{QO} = \frac{1}{2}(S_{even} + S_{odd}) \qquad [7]$$

and

$$S_{DQ} = -\frac{1}{2}(S_{even} - S_{odd}), \qquad [8]$$

respectively.

Denoting the amplitude of the MQ signal for rank ℓ and coherence order m as $A_{\ell m}$ (*1, 11*), amplitudes of S_{QO} and S_{DQ} may be expressed as

$$\text{amplitude of } S_{QO} = \frac{3}{4}A_{20} \qquad [9]$$

and

$$\text{amplitude of } S_{DQ} = -\frac{1}{4}A_{22} + A_{32}, \qquad [10]$$

where the factors for the second-rank components, i.e., $\frac{3}{4}$ and $-\frac{1}{2}$, are described elsewhere (*8, 12*).

From Eqs. [7] through [10], S_{even} and S_{odd} may be written as

$$S_{even} = \frac{3}{4}A_{20} - (A_{32} - \frac{1}{4}A_{22}) \qquad [11]$$

and

$$S_{odd} = \frac{3}{4}A_{20} + (A_{32} - \frac{1}{4}A_{22}). \qquad [12]$$

If relaxation during the short evolution time is neglected, we may assume that

$$A_{20} = A_{22}. \qquad [13]$$

Then, Eqs. [11] and [12] may be rewritten as

$$S_{even} = A_{20} - A_{32} \qquad [14]$$

and

$$S_{odd} = \frac{1}{2}A_{20} + A_{32}. \qquad [15]$$

TABLE 2
RF Phases and Flip Angles for J–B and DQF-4 Sequences

	ϕ_P	ϕ_E	ϕ_R	θ_3	θ_4
J–B	$(k + \frac{1}{2})\pi$	$\frac{n}{2}\pi$	0	$\frac{1}{4}\pi$	$\frac{1}{4}\pi$
DQF-4	$(k + \frac{1}{2})\pi$	$\frac{n}{2}\pi$	$n\pi$	$\frac{1}{4}\pi$	$\frac{1}{4}\pi$

TABLE 3
Phase Lists (in Units of 90°) for Various MQF Schemes Based on the Pulse Sequence [1]

RF	S_{odd}	S_{even}	J-B	DQF-4
$(90°, \phi_1)$	3113 3113 1331 1331	0220 0220 2002 2002	0231 2013 0231 2013 2013 0231 2013 0231	0123 0321 2301 2103
$(180°, \phi_2)$	0000 2222 1111 3333	0000 2222 1111 3333	0000 0000 2222 2222 1111 1111 3333 3333	0123 0321 0123 0321 1230 1032 1230 1032 2301 2103 2301 2103 3012 3210 3012 3210
$(45°, \phi_3)$	2200	1133	1122 3300	1230 1032 1230 1032
$(45°, \phi_4)$	1	1	1	1
ϕ_R	02	02	20	0202 0202 2020 2020 2020 2020 0202 0202

Furthermore, the DQ signal of DQF-4, in contrast to that of DQF-1, varies smoothly with θ_3 and θ_4 as $\sin(2\theta_3)$ and $\sin(2\theta_4)$, respectively (*12*). This also holds for J–B, due to $d_{01}^2(\theta_3) = \frac{1}{2}\sqrt{\frac{3}{2}}\sin(2\theta_3)$ and $d_{10}^2(\theta_4) = \frac{1}{2}\sqrt{\frac{3}{2}}\sin(2\theta_4)$ (*11*). Therefore, both QO and DQ signals have the same functional dependence on the RF flip angles, and hence, the linear superposition of these signals will not be altered by RF field inhomogeneity.

EXPERIMENTAL RESULTS

The above methods have been experimentally verified by use of a phantom consisting of hydrated bovine cartilage soaked into 100 mM NaCl solution (*9*). The NMR system was a Bruker AM-300 (7.05 T) with an on-resonance carrier frequency (*13*). Experimental parameters were $\tau_P = 4$ ms, $\tau_E = 0.1$ ms, number of accumulations = 192, and repetition time = 400 ms (*14*). The phase cycling employed for the various MQFs is listed in Table 3.

The acquired spectra corresponding to S_{even} and S_{odd} are shown in Figs. 1A and 1B, respectively. With the preparation time employed, A_{32} is greater than A_{20} because the evolution from first rank to third rank is greater than that from first rank to second rank during the preparation time. This results in the negative spectral peak of Fig. 1A in accordance with Eq. [14]. Also, note the enhanced spectral amplitude of Fig. 1B due to the constructive interference between the second and third-rank components as in Eq. [15].

From S_{even} and S_{odd}, the QO and DQ signals were abstracted by use of Eqs. [7] and [8], and the corresponding spectra are shown in Figs. 1C and 1D. Transverse relaxation times for the second-rank component are relatively shorter than those for the third-rank component, resulting in QO spectra broader than DQ spectra (*9*). In the DQ spectra corresponding to DQF-4, the contribution of the second-rank component is 25% of the maximum attainable second-rank component as in Eq. [10], making the DQ spectra mostly a third-rank component in this case.

The simultaneous acquisition of QO and DQ signals was confirmed by separately acquiring QO and DQ spectra (Figs. 1E and 1F, respectively) by direct use of their individual
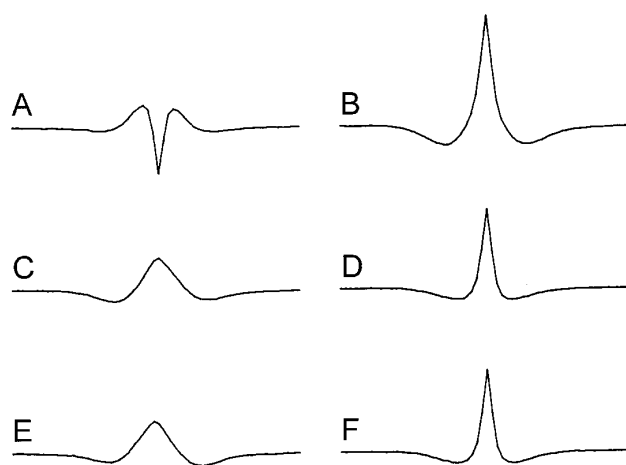
FIG. 1. MQ spectra acquired from a phantom consisting of bovine cartilage soaked into 100 mM NaCl. (A) S_{even}, (B) S_{odd}, (C) $S_{QO} = \frac{1}{2}(S_{even} + S_{odd})$, (D) $S_{DQ} = -\frac{1}{2}(S_{even} - S_{odd})$, (E) J-B, (F) DQF-4. The scales for the frequency and amplitude axes are the same for all the spectra. The peak amplitudes of spectra (A) to (F) are −1.2, 2.7, 0.8, 1.9, 0.8, and 2.0.
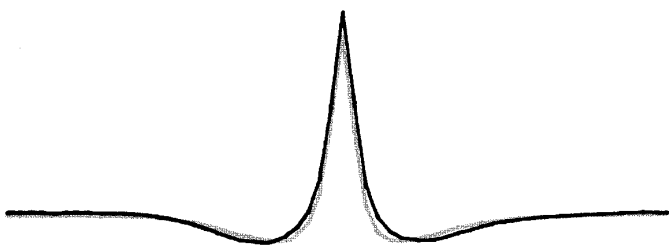
FIG. 2. The spectrum corresponding to the third-rank DQ component, i.e., $A_{32} = -\frac{1}{3}(S_{even} - 2S_{odd})$. For a comparison, the spectrum of S_{DQ} is overlaid with a lower gray level. The spectral peak amplitude for A_{32} is 2.2.

filtering schemes, i.e., J–B and DQF-4. Note that the spectra of Figs. 1C and 1D match well with the corresponding spectra of Figs. 1E and 1F.

Furthermore, if relaxation during the short evolution time can be neglected, second- and third-rank components can be abstracted from Eqs. [14] and [15] as

$$A_{20} = \frac{2}{3}(S_{even} + S_{odd}) \qquad [16]$$

and

$$A_{32} = -\frac{1}{3}(S_{even} - 2S_{odd}). \qquad [17]$$

Compared with S_{QO} in Eq. [7], A_{20} in Eq. [16] is the scaled version of S_{QO}. From S_{even} and S_{odd} in Fig. 1, the third-rank component was abstracted by use of Eq. [17], and its spectrum is shown in Fig. 2, where it is also compared with that for S_{DQ}. Since second- and third-rank DQ signals interfere destructively in S_{DQ} as in Eq. [10], the absence of a second-rank component in A_{32} results in an increase of the spectral peak amplitude relative to that of S_{DQ}.

CONCLUSIONS

Both QO and DQ signals can be generated simultaneously by the same RF sequence without any loss in signal amplitude. In addition, the acquired MQ signals can be readily decomposed into their second- and third-rank components, i.e., into quadrupolar order and biexponential relaxation components. This allows us to reduce considerably the scanning time necessary to acquire MQ signals of different coher-

ence orders and ranks, which should prove particularly helpful for *in vivo* studies. We propose the acronym ''SAMQ,'' *s*imultaneous *a*cquisition of *MQ* signals, for the technique described here.

REFERENCES

1. G. Jaccard, S. Wimperis, and G. Bodenhausen, Multiple-quantum NMR spectroscopy of $S = 3/2$ spins in isotropic phase: A new probe for multiexponential relaxation, *J. Chem. Phys.* **85**, 6282–6293 (1986).

2. W. D. Rooney and C. S. Springer Jr., The molecular environment of intracellular sodium: ^{23}Na NMR relaxation, *NMR Biomed.* **4**, 227–245 (1991).

3. G. S. Payne, A.-M. L. Seymour, P. Styles, and G. K. Radda, Multiple quantum filtered ^{23}Na NMR spectroscopy in the perfused heart, *NMR Biomed.* **3**, 139–146 (1990).

4. J. L. Allis, A.-M. L. Seymour, and G. K. Radda, Absolute quantification of intracellular Na$^+$ using triple-quantum-filtered sodium-23 NMR, *J. Magn. Reson.* **93**, 71–76 (1991).

5. R. B. Hutchison, J. J. A. Huntley, H. Z. Zhou, D. J. Ciesla, and J. I. Shapiro, Changes in double quantum filtered sodium intensity during prolonged ischemia in the isolated perfused heart, *Magn. Reson. Med.* **29**, 391–395 (1993).

6. R. C. Lyon and A. C. McLaughlin, Double-quantum filtered ^{23}Na NMR study of intracellular sodium in the perfused liver, *Biophys. J.* **67**, 369–376 (1994).

7. V. D. Schepkin, I. O. Choy, and T. F. Budinger, Sodium alterations in isolated rat heart during cardioplegic arrest, *J. Appl. Physiol.* **81**(6), 2696–2702 (1996).

8. R. Kemp-Harper and S. Wimperis, Detection of the interaction of sodium ions with ordered structures in biological systems. Use of the Jeener–Broekaert experiment, *J. Magn. Reson. B* **102**, 326–331 (1993).

9. U. Eliav and G. Navon, Analysis of double-quantum-filtered NMR spectra of ^{23}Na in biological tissues, *J. Magn. Reson. B* **103**, 19–29 (1994).

10. R. Reddy, L. Bolinger, M. Shinnar, E. Noyszewski, and J. S. Leigh, Detection of residual quadrupolar interaction in human skeletal muscle and brain in vivo via multiple quantum filtered sodium NMR spectra, *Magn. Reson. Med.* **33**, 134–139 (1995).

11. N. Müller, G. Bodenhausen, and R. R. Ernst, Relaxation-induced violations of coherence transfer selection rules in nuclear magnetic resonance, *J. Magn. Reson.* **75**, 297–334 (1987).

12. K. J. Jung, J. S. Tauskela, and J. Katz, New double-quantum filtering schemes, *J. Magn. Reson. B* **112**, 103–110 (1996).

13. K. J. Jung and J. Katz, Chemical-shift-selective acquisition of multiple-quantum-filtered ^{23}Na signal, *J. Magn. Reson. B* **112**, 214–227 (1996).

14. K. J. Jung and J. Katz, Mathematical analysis of generation and elimination of intersequence stimulated echo in double-quantum filtering, *J. Magn. Reson.* **124**, 232–236 (1997).